

PACS numbers: 07.07.Df, 07.60.Pb, 78.20.Ci, 78.30.Jw, 78.40.Me, 78.67.Sc, 82.35.Np

Synthesis of PVA/PVP/SnO₂ Nanocomposites: Structural, Optical, and Dielectric Characteristics for Pressure Sensors

Ahmed Hashim¹, Alaa J. Kadham Algidsawi², Hind Ahmed¹,
Aseel Hadi³, and Majeed Ali Habeeb¹

¹*Department of Physics, College of Education of Pure Sciences,
University of Babylon,
Babylon, Iraq*

²*Department of Soil and Water, College of Agriculture,
AL-Qasim Green University,
Babylon, Iraq*

³*University of Babylon, College of Materials Engineering,
Department of Ceramic and Building Materials,
Babylon, Iraq*

Nanocomposites' films are prepared from PVA/PVP blend with various ratios of SnO₂ by using the casting method. The structural, optical, and dielectric characteristics of nanocomposites are studied for pressure sensors' applications. The results indicate to the optical characteristics of PVA/PVP/SnO₂ nanocomposites improved with the rise in SnO₂-nanoparticles' ratios. The dielectric characteristics show that the dielectric parameters of PVA/PVP blend enhance with rise in SnO₂-nanoparticles' ratios. The pressure-sensor results for nanocomposites show that the capacitance increases with an increase in pressure.

Плівки нанокompозитів готуються з суміші ПВА/ПВП з різними співвідношеннями SnO₂ за допомогою методи лиття. Структурні, оптичні та діелектричні характеристики нанокompозитів вивчаються задля застосування давачів тиску. Результати вказують на те, що оптичні характеристики нанокompозитів ПВА/ПВП/SnO₂ поліпшилися зі зростанням співвідношення наночастинок SnO₂. Діелектричні характеристики показують, що діелектричні параметри суміші ПВА/ПВП поліпшуються зі зростанням співвідношення наночастинок SnO₂. Результати давача тиску для нанокompозитів показують, що ємність збільшується зі збільшенням тиску.

Key words: pressure sensors, tin oxide, energy gap, conductivity, dielectric properties.

Ключові слова: сенсори тиску, оксид Стануму, енергетична щільність, провідність, діелектричні властивості.

(Received 30 May, 2020; in revised form, 19 June, 2020)

1. INTRODUCTION

In recent years, the electrical and optical characteristics' studies of polymers include attracted greatly attention in their approaches' view in devices (optical, electronic ones). The electrical characteristics are aimed to know the charge transport prevalent nature in these substances, while the optical characteristics are aimed to anti-reflection, achieving better reflection and polarization characters. Optical and electrical characteristics of the polymers may be suitably customized by the dopant addition, depending on their reactivity with the polymer matrix. Moreover, the polymer materials advantages such as good mould ability, high strength and flexibility might be combined with the great characteristics of inorganic substances like heat stability, heat strength, high strength, and chemical resistance during producing composite substances. The large-range fields of nanofillers like filters, tissue engineering, catalysis, scaffold, sensors and wound dressing might be extended with improving their electrical, mechanical, magnetic, optical, and thermal characteristics by incorporating organic and inorganic constituents in their structures [1].

The creation of polymer composites by means of polymer matrix, which can offer high tensile strength and non-toxicity, will be appropriate for food packaging and biomedical applications. Polyvinyl alcohol (PVA) offers the property of biocompatibility, non-toxicity, water solubility, superior tensile strength and is gradually replacing other non-biocompatible plastics like polyethylene, polypropylene, HDPE, *etc.* in many fields [2].

Polyvinyl alcohol is semi-crystalline, with low electrical conductivity. PVA has certain physical characteristics resultant from crystal/amorphous interfacial effects. Its electrical characteristics may be modified to an exact requirement by the suitable doping substance addition [3]. Poly(N-vinylpyrrolidone) (PVP) attracts particular attention between the polymers that is related to its excellent stability of environmental, appropriate electrical conductivity and easy processability. The reactive pyrrolidone group of PVP easily forms complexes with many inorganic salts, synthetic or natural functional polymers, biomolecules and biomacromolecules [4].

Improved characteristics of semiconducting metal oxides create them to find approaches in several applications. Between the semiconducting metal oxides, tin oxide (SnO_2) has been generally inves-

tigated due to its large band gap of 3.6 eV and its potential fields in different approaches like liquid-crystal displays, gas sensors, photovoltaic cells, and solar cells [5]. SnO₂-nanostructures' multifunctionality arises relating to their large band gap, high surface to volume ratio, high exciton binding energy of 130 meV at room temperature (300 K), variation of remarkable resistivity in gaseous environment, chemical, mechanical and thermal stabilities, *etc.* Optoelectronic characteristics of SnO₂ depend on the impurities' presence and its stoichiometry with respects to oxygen [6].

2. MATERIALS AND METHODS

PVA-PVP-SnO₂ nanocomposites were prepared by casting technique. The solution of polymers was prepared by dissolving of 0.5 gm of PVP + PVA in distilled water (20 ml) with ratio 77 wt.% PVA:23 wt.% PVP. The SnO₂ nanoparticles were added to blend solution with ratios 1.5, 3 and 4.5 wt.%. The optical characteristics were tested in wavelength range 220–820 nm by using spectrophotometer (UV/1800/Shimadzu). The dielectric characteristics were measured in frequency range 100 Hz–5 MHz by LCR meter type (HIOKI 3532-50 LCR HI TESTER). The pressure-sensor application was tested by measuring the parallel capacitance (C_p) between two electrodes on the top and bottom of film with different pressures' range 80–200 bar. Absorption coefficient, α , is given by [7, 8]:

$$\alpha = 2.303A/t; \quad (1)$$

A is absorbance, and t is sample thickness. The energy gap is determined by the equation [9, 10]

$$Ah\nu = B(h\nu - E_g)^r, \quad (2)$$

where B is constant, $h\nu$ is photon energy, E_g is energy gap, $r = 3$ for forbidden indirect transition, and $r = 2$ is allowed indirect transition. Refractive index, n , is given by the equation [11]

$$n = (1 + \sqrt{R}) / (1 - \sqrt{R}); \quad (3)$$

here, R is reflectance. The extinction coefficient, k , is defined by

$$k = \alpha\lambda / (4\pi), \quad (4)$$

where λ is wavelength [12]. The parts of dielectric constant, real, ϵ_1 , and imaginary, ϵ_2 , ones are calculated by [13]:

$$\epsilon_1 = n^2 - k^2, \quad (5)$$

$$\varepsilon_2 = 2nk. \quad (6)$$

The optical conductivity, σ_{op} , may be calculated by the equation [14, 15]

$$\sigma_{op} = \alpha nc / (4\pi). \quad (7)$$

The dielectric constant, ε' , is given by [16]:

$$\varepsilon' = C_p / C_o \quad (8)$$

where C_p is capacitance and C_o is capacitance of vacuum. The dielectric loss, ε'' , can be calculated by using [17]:

$$\varepsilon'' = \varepsilon' D, \quad (9)$$

where D is dispersion factor. The A.C. conductivity can be determined by using [18]:

$$\sigma_{ac} = \omega \varepsilon'' \varepsilon_o, \quad (10)$$

where ω is angular frequency.

3. RESULTS AND DISCUSSION

Figure 1 explains the FTIR test of nanocomposites. The FTIR tests of PVA/PVP/SnO₂ nanocomposites show the nanocomposites' interactions. From Figure 1, it is seen bands at around 3256 cm⁻¹, which are related to OH groups. The peaks at around 1652 cm⁻¹ are due to C=O groups. The bands at around 1290 cm⁻¹ are due to the other bonds (C-O-C) [19, 20].

Figure 2 represents the absorbance variation of blend with wavelength. The absorbance of blend rises with rising of the SnO₂-nanoparticles' ratios that is due to the rise in number of charge carries in nanocomposites [21–26], as exposed in Fig. 3, which shows the SnO₂-nanoparticles' distribution in PVA/PVP blend. The absorption-coefficient variation with energy of photon is shown in Fig. 4. Absorption coefficient of PVA/PVP blend rise with rising of the SnO₂ nanoparticles' ratios that is related to rise of the absorbance [27]. The absorption coefficient shows the nature of energy gap. From the α values, the energy gap is indirectly corresponding, as shown in Figs. 5 and 6, to allowed and forbidden transitions, respectively. The energy gap for transitions (allowed and forbidden ones) is reduced with rise in SnO₂-nanoparticles' ratios that is related to creating the localized levels in the optical band gap [28, 29].

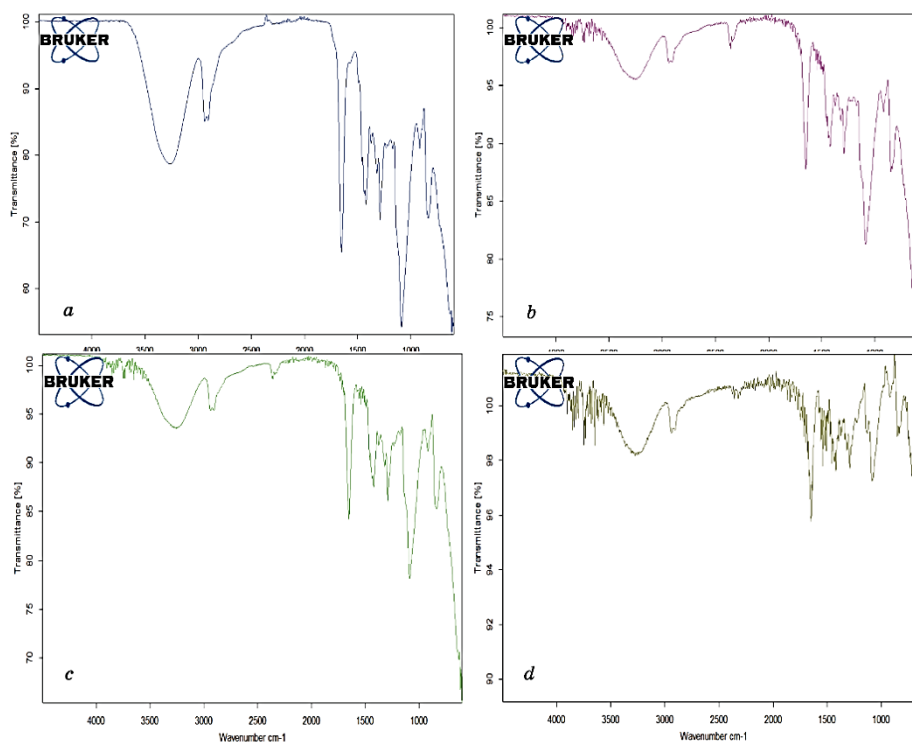


Fig. 1. FTIR test of PVA/PVP/SnO₂ nanocomposites: *a*—blend; *b*—1.5 wt.% SnO₂; *c*—3 wt.% SnO₂; *d*—4.5 wt.% SnO₂.

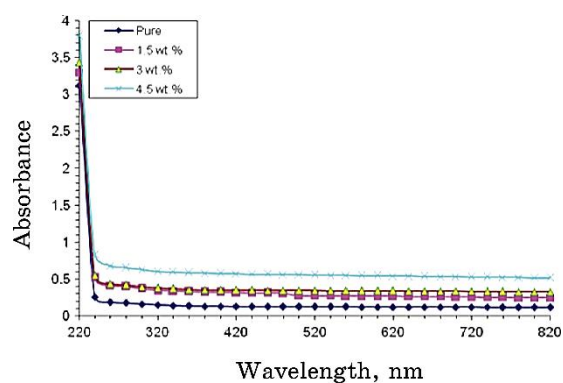


Fig. 2. Relationship between the absorbance of PVA–PVP blend and wavelength.

The variations of n and k with wavelength are shown in Figs. 7 and 8, respectively. The refractive index and extinction coefficient are increased with rise in SnO₂ content that is due to rise in absorp-

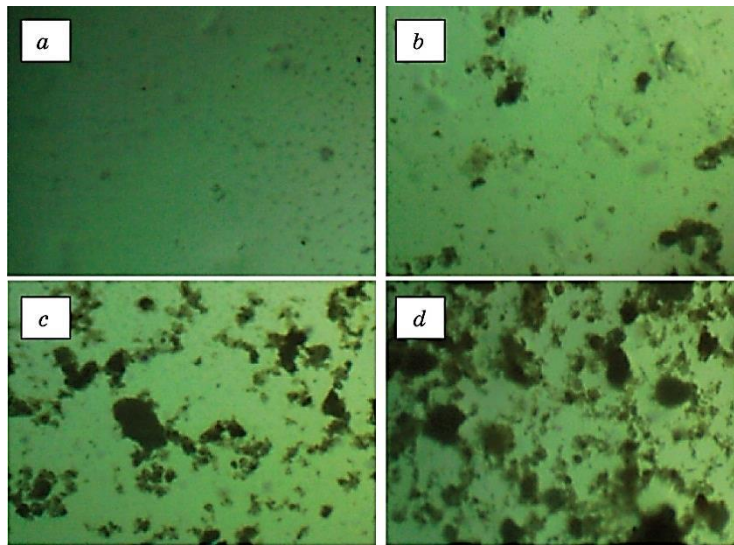


Fig. 3. Microscope images of PVA/PVP/SnO₂ nanocomposites: *a*—blend; *b*—1.5 wt.% SnO₂; *c*—3 wt.% SnO₂; *d*—4.5 wt.% SnO₂.

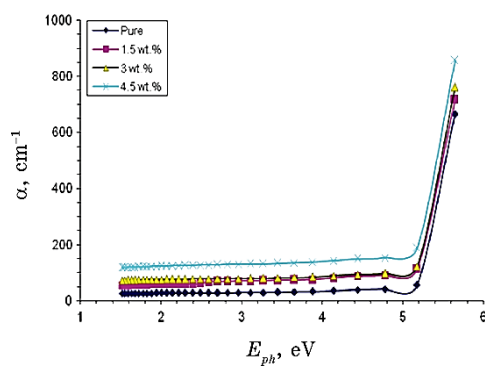


Fig. 4. Absorption-coefficient variation with energy of photon.

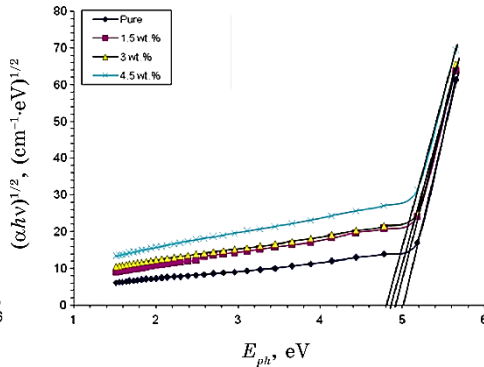


Fig. 5. Energy gap for allowed indirect transitions.

tion and density of nanocomposite [30].

Figures 9 and 10 show the variations of ϵ_1 and ϵ_2 of PVA/PVP/SnO₂ with wavelength, respectively. ϵ_1 and ϵ_2 rise with rise in SnO₂ that is related to the real part dependent on n^2 because the values of k^2 are small as compared to values of n^2 , while imaginary part mainly depends on the values of extinction coefficient [31].

Figure 11 explains the optical conductivity variation for PVA/PVP/SnO₂ films with wavelength.

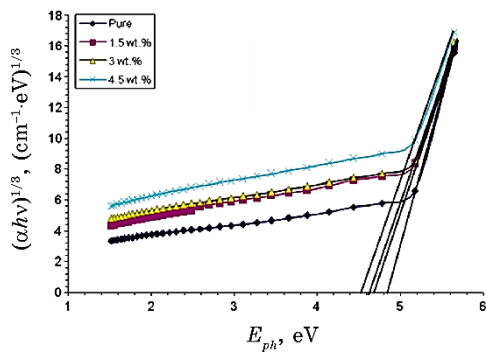


Fig. 6. Energy gap for forbidden indirect transitions.

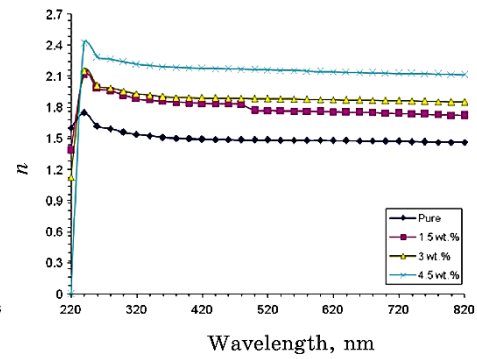


Fig. 7. Variation of refractive index with wavelength.

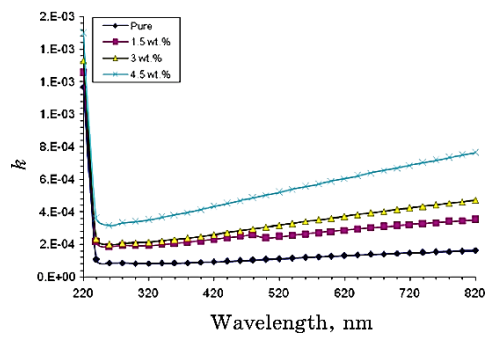


Fig. 8. Variation of extinction coefficient with wavelength.

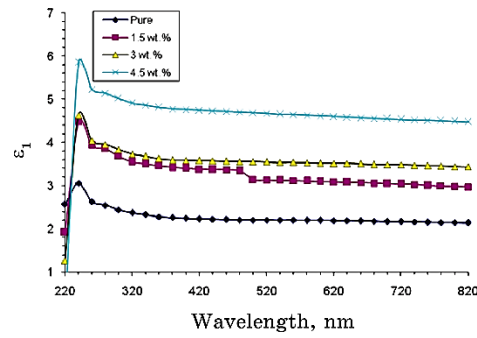


Fig. 9. Variation of ϵ_1 for PVA/PVP/SnO₂ with wavelength.

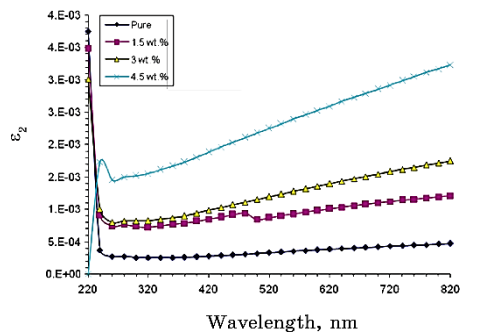


Fig. 10. Variation of ϵ_2 for PVA/PVP/SnO₂ with wavelength.

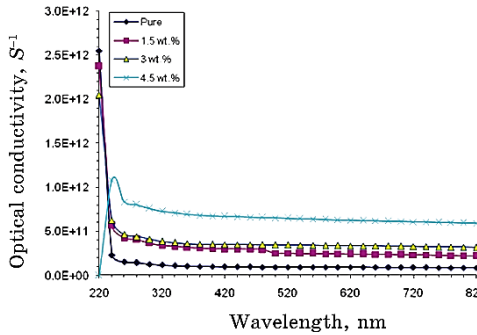


Fig. 11. Optical conductivity variation for PVA/PVP/SnO₂ nanocomposites with wavelength.

The optical conductivity of PVA/PVP blend increases with rise in

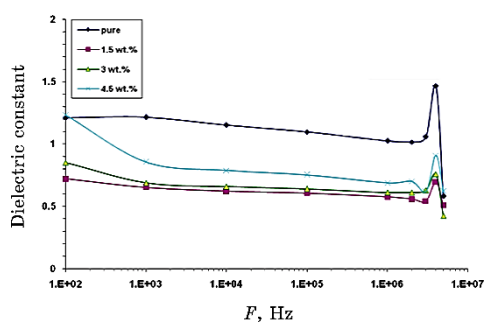


Fig. 12. Relationship between dielectric constant and frequency.

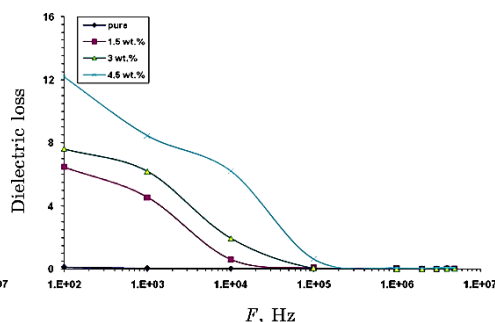


Fig. 13. Relationship between dielectric loss and frequency.

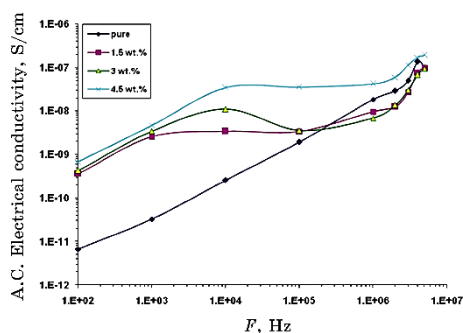


Fig. 14. Relationship between A.C. electrical conductivity and frequency.

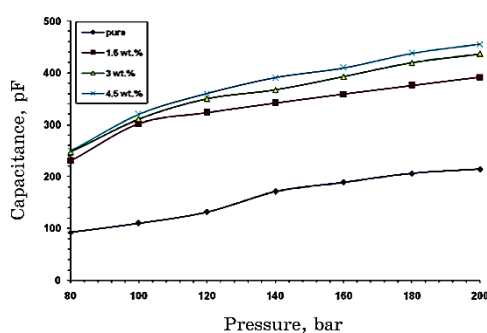


Fig. 15. Variation of capacitance for nanocomposites with pressure.

SnO_2 -nanoparticles' ratios that is attributed to decrease in energy band gap and rise in the α and n values [32–35].

Figures 12–14 show the relationship between ϵ' , ϵ'' , $\sigma_{\text{A.C.}}$ and frequency, respectively. The dielectric parameters of PVA/PVP blend rise with rising of SnO_2 ratios that is due to increase of the charge-carriers' density in blend [36]. The dielectric constant and loss also increase, while the conductivity decreases with rise in frequency; this behaviour is related to polarization effects [37, 38].

Figure 15 shows the capacitance variation for nanocomposites' samples with pressure (compression stress). As from Figure 15, the capacitance increases with increase in pressure. This behaviour may be due to the crystal consisting of many interlocking domains, which contain negative and positive charges. These domains are symmetrical inside the crystal with the result that the crystal has a net charge of zero. When a pressure is applied to the crystal, this symmetry is broken, and in order to restore the symmetry, these domains realign themselves, and through the realignment, generate

a current that causes the increase in capacitance [39].

4. CONCLUSIONS

The results indicate to the optical characteristics of PVA/PVP blend, which are improved with a rise in tin oxide content.

The dielectric properties show that the dielectric parameters enhance with rising of the SnO₂-nanoparticles' ratios.

The results of pressure sensors indicate that the PVA/PVP/SnO₂ nanocomposites have excellent sensitivity for pressure.

REFERENCES

1. G. M. Nasr, A. S. Abd El-Haleem, A. Klingner, A. M. Alnozahy, and M. H. Mourad, *J. of Multidisciplinary Eng. Sci. and Technology*, **2**, Iss. 5: 884 (2015).
2. K. Gulati, S. Lal, P. K. Diwan, and S. Arora, *Int. J. of Appl. Eng. Res.*, **14**, No. 1: 170 (2019).
3. G. V. Kumar, *Int. J. of Res. - Granthaalayah*, **5**, Iss. 4 (RAST): 87 (2017); DOI: [10.5281/zenodo.803434](https://doi.org/10.5281/zenodo.803434)
4. U. Bunyatova, Z. M. O. Rzayev, and M. Şimşek, *eXPRESS Polymer Letters*, **10**, No. 7: 598 (2016).
5. S. M. Priya, A. Geetha, and K. Ramamurthi, *J. Sol-Gel Sci. Technol.*, **78**, Iss. 2: 365 (2016); doi:[10.1007/s10971-016-3966-7](https://doi.org/10.1007/s10971-016-3966-7)
6. S. Sarmah and A. Kumar, *Indian J. Phys.*, **84**, No. 9: 1211 (2010).
7. A. Hashim, M. A. Habeeb, A. Khalaf, and A. Hadi, *Sensor Letters*, **15**: 589 (2017); <https://doi.org/10.1166/sl.2017.3856>
8. A. Hashim and M. A. Habeeb, *Transactions on Electrical and Electronic Materials*, **20**: 107 (2019); doi:[10.1007/s42341-018-0081-1](https://doi.org/10.1007/s42341-018-0081-1)
9. A. Hashim and M. A. Habeeb, *J. of Bionanoscience*, **12**, No. 5: 660 (2018); <https://doi.org/10.1166/jbns.2018.1578>
10. Q. M. Jebur, A. Hashim, M. A. Habeeb, *Transactions on Electrical and Electronic Materials*, **20**: 334 (2019); <https://doi.org/10.1007/s42341-019-00121-x>
11. Q. M. Jebur, A. Hashim, and M. A. Habeeb, *Egypt. J. Chem.*, **63**, Iss. 3: 611 (2020); doi:[10.21608/EJCHEM.2019.10197.1669](https://doi.org/10.21608/EJCHEM.2019.10197.1669)
12. F. L. Rashid, A. Hashim, M. A. Habeeb, S. R. Salman, and H. Ahmed, *Journal of Engineering and Applied Sciences*, **8**, No. 5: 137 (2013).
13. N. Hayder, M. A. Habeeb, and A. Hashim, *Egypt. J. Chem.*, **63**, Special Issue (Part 2) Innovation in Chemistry: 1 (2020); doi:[10.21608/ejchem.2019.14646.1887](https://doi.org/10.21608/ejchem.2019.14646.1887)
14. H. Ahmed, H. M. Abduljalil, and A. Hashim, *Transactions on Electrical and Electronic Materials*, **20**: 218 (2019); <https://doi.org/10.1007/s42341-019-00111-z>
15. H. Ahmed, H. M. Abduljalil, and A. Hashim, *Transactions on Electrical and Electronic Materials*, **20**: 206 (2019); <https://doi.org/10.1007/s42341-019-00100-2>
16. A. Hashim, M. A. Habeeb, A. Hadi, Q. M. Jebur, and W. Hadi, *Sensor Let-*

- ters, **15**: 998 (2017); doi:10.1166/sl.2018.3935
17. M. A. Habbeb, A. Hashim, Abdul-Raheem K. AbidAli, *European Journal of Scientific Research*, **61**, No. 3: 367 (2011).
 18. B. Hussien, A. K. Algidsawi, and A. Hashim, *Australian Journal of Basic and Applied Sciences*, **5**, No. 7: 933 (2011).
 19. A. Hashim, I. R. Agool, and K. J. Kadhim, *Journal of Materials Science: Materials in Electronics*, **29**, Iss. 12: 10369 (2018); <https://doi.org/10.1007/s10854-018-9095-z>
 20. I. R. Agool, K. J. Kadhim, and A. Hashim, *International Journal of Plastics Technology*, **21**, Iss. 2: 444 (2017); <https://doi.org/10.1007/s12588-017-9196-1>
 21. M. A. Habeeb, A. Hashim, and A. Hadi, *Sensor Letters*, **15**, No. 9: 785 (2017); doi:10.1166/sl.2017.3877
 22. F. A. Jasim, F. Lafta, A. Hashim, M. Ali, and A. G. Hadi, *Journal of Engineering and Applied Sciences*, **8**, No. 5: 140 (2013); DOI: 10.36478/jeasci.2013.140.142
 23. N. H. Al-Garah, F. L. Rashid, A. Hadi, and A. Hashim, *Journal of Bionanoscience*, **12**: 336 (2018); doi:10.1166/jbns.2018.1538
 24. F. A. Jasim, A. Hashim, A. G. Hadi, F. Lafta, S. R. Salman, and H. Ahmed, *Research Journal of Applied Sciences*, **8**, Iss. 9: 439 (2013).
 25. A. Hashim and Z. S. Hamad, *J. of Bionanoscience*, **12**, No. 4: 504 (2018); doi:10.1166/jbns.2018.1561
 26. A. Hashim and N. Hamid, *Journal of Bionanoscience*, **12**, No. 6: 788 (2018); doi:10.1166/jbns.2018.1591
 27. A. Hashim and A. Jassim, *Sensor Letters*, **15**, No. 12: 1003 (2017); doi:10.1166/sl.2018.3915
 28. A. Hashim, M. A. Habeeb, and A. Hadi, *Sensor Letters*, **15**, No. 9: 758 (2017); doi:10.1166/sl.2017.3876
 29. A. Hashim and A. Jassim, *Journal of Bionanoscience*, **12**: 170 (2018); doi:10.1166/jbns.2018.1518
 30. I. R. Agool, F. S. Mohammed, and A. Hashim, *Advances in Environmental Biology*, **9**, No. 11: 1 (2015).
 31. A. Hashim and Q. Hadi, *Journal of Materials Science: Materials in Electronics*, **29**: 11598 (2018); <https://doi.org/10.1007/s10854-018-9257-z>
 32. A. Hashim, Y. Al-Khafaji, and A. Hadi, *Transactions on Electrical and Electronic Materials*, **20**: 530 (2019); <https://doi.org/10.1007/s42341-019-00145-3>
 33. D. Hassan and A. Hashim, *J. of Bionanoscience*, **12**, Iss. 3: (2018); doi:10.1166/jbns.2018.1533
 34. D. Hassan and A. Hashim, *J. of Bionanoscience*, **12**, Iss. 3: 346 (2018); doi:10.1166/jbns.2018.1537
 35. A. Hashim and Z. S. Hamad, *J. of Bionanoscience*, **12**, No. 4: 488 (2018); doi:10.1166/jbns.2018.1551
 36. A. Hashim and Q. Hadi, *Sensor Letters*, **15**, No. 11: 951 (2017); doi:10.1166/sl.2017.3892
 37. D. Hassan and A. H. Ah-Yasari, *Bulletin of Electrical Engineering and Informatics*, **8**, Iss. 1: 52 (2019); doi:10.11591/eei.v8i1.1019
 38. A. Hashim and A. Hadi, *Ukrainian Journal of Physics*, **63**, No. 8: 754 (2018); <https://doi.org/10.15407/ujpe63.8.754>
 39. A. Hashim and A. Hadi, *Sensor Letters*, **15**, No. 12: 1019 (2017); doi:10.1166/sl.2017.3910